JOC*Article*

A Highly Selective Rearrangement of a Housane-Derived Cation Radical: An Electrochemically Mediated Transformation

Young Sam Park,[†] Selina C. Wang,[‡] Dean J. Tantillo,[‡] and R. Daniel Little*[,†]

Department of Chemistry & Biochemistry, University of California, Santa Barbara, California 93106, and Department of Chemistry, University of California, Davis, California 95616

little@chem.ucsb.edu

Received January 30, 2007

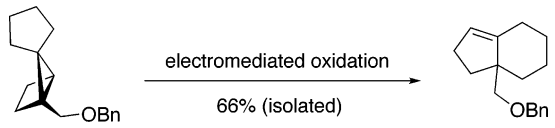

18 **23**

To utilize housane-derived cation radicals as intermediates for the synthesis of the bicyclo (*n*.3.0) framework of natural products, a highly regioselective [1,2] shift of carbon to either a radical or an electron-deficient site is required. Herein we describe how this has been accomplished, provide a set of guidelines to assess housane oxidizability prior to its synthesis, and describe a synthesis of housane **18** that capitalizes upon the facility of [1,5] hydrogen shifts in substituted cyclopentadienes. The catalytic electrochemically mediated oxidation of **18** leads to a cation radical that engages in a rearrangement leading to the (4.3.0) adduct **23**. The appearance of a catalytic current in the cyclic voltammogram of a solution containing the tris(aryl)amine and housane **18** is an excellent indicator that the amminium cation radical $\mathbf{14}^{\bullet+}$ is able to oxidize the housane and return the mediator to the original redox couple. DFT calculations show electron density on both the aryl and strained σ framework in the HOMO of housane **18**. From the spin density and electrostatic potential map for the cation radical, a picture where the spin resides on the side that is distal to the substituent emerges, while the hole is proximal to it. Both experiment and theory show that the rearrangement is best characterized as a [1,2] carbon shift toward an electron-deficient site and that migration toward the substituent-bearing carbon is much preferred over the alternative pathway.

Introduction

We recently described the rearrangement of the cation radicals derived from housanes **1**−**3** and **7**.[1] Surprisingly, each of the 2-aryl-substituted systems, **1**−**3**, rearranged with modest selectivity, favoring the product of housane ring opening with the subsequent migration of the labeled methylene group toward the bridgehead carbon positioned distal to the aryl substituent (viz. toward Cα′). We attributed the selectivity to the existence of a bridging interaction between the aryl group and the cation radical (see **6**, Scheme 1), much the way a phenyl group bridges when stabilizing a vicinal carbocation.[2] Nearly the same level of selectivity and same preference for a distal migration was observed regardless of the electron demand of the para substituent appended to the aryl group. Thus, the product ratio is 72:28 when it is methoxy and 80:20 when it is carboethoxy, a result that is consistent with the stabilization of a bridgehead radical rather than a carbocation.

In contrast to these cases, no selectivity was observed in the rearrangement of the cation radical derived from the 2-trimethylsilylmethyl-substituted housane **7** (Scheme 2); nearly equal amounts of **8** and **9** were produced despite the possibility that γ-silyl stabilization of a cation at Cα could have biased the regiochemical outcome.[3]

While fundamentally interesting, these results are unsatisfactory if one wishes to apply the chemistry to the synthesis of specific structures. One of our objectives, for example, is to use the transformation in the manner illustrated by the conver-

[†] University of California, Santa Barbara.
[‡] University of California, Davis.

(1) Gerken, J. B.; Wang, S. C.; Preciado, A. B.; Park, Y. S.; Nishiguchi, G.; Tantillo, D. J.; Little, R. D. *J. Org. Chem.* **2005**, *70*, 4598−4608.

(2) Cram, D. J. *J. Am. Chem. Soc.* **1964**, *86*, 3767−3772.

(3) (a) For a review concerning the interaction of silicon with positively charged carbon at the α, β, γ, and δ positions, see: Lambert, J. B. *Tetrahedron* **1990**, *46*, 2677−2689. (b) Kaimakliotis, C; Fry, A. J. *J. Org. Chem.* **2003**, *68*, 9893−9898; reports a novel silicon γ-aryl effect upon redox potential.

10.1021/jo070190x CCC: $37.00
Published on Web 05/11/2007

SCHEME 1. Aryl Bridging in the Rearrangement of 2-Aryl-Substituted Housanes

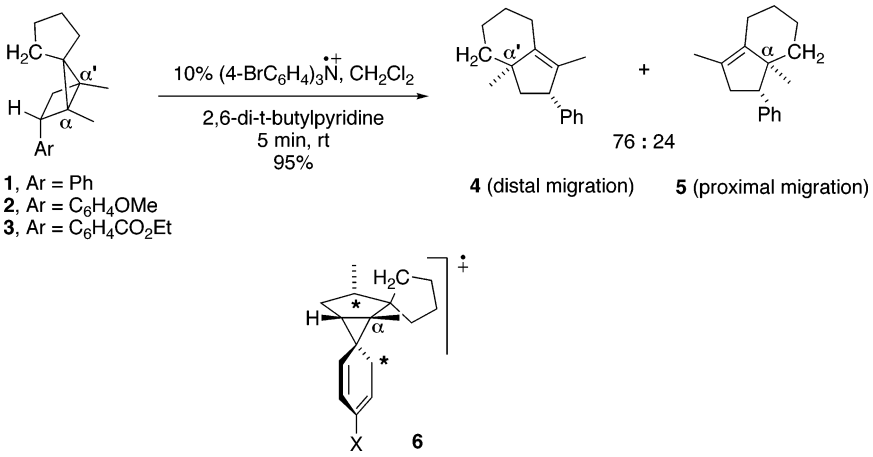

SCHEME 2. The Presence of a γ-Silyl Substituent Affords No Regioselectivity

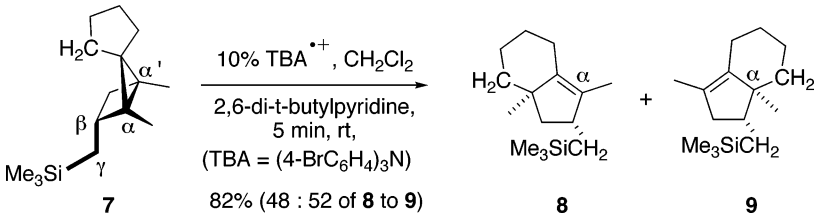

SCHEME 3. Idealized Transformation Leading to the Bicyclo (*n*.3.0) Framework

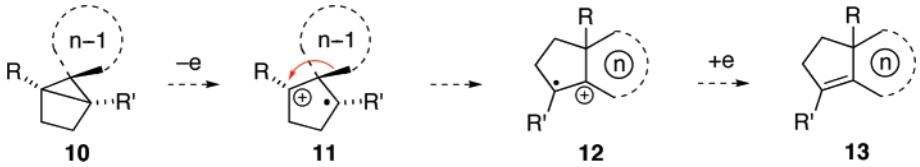

sion of **10** (R ≠ R′) to **13** in order to access the bicyclo (*n*.3.0) framework that is common to a variety of natural products (Scheme 3).[4] To do so clearly requires a solution to the regiochemical control issue; significantly greater preferences must be achieved.

Herein we (a) provide a solution to the problem of regiochemical control and describe (b) qualitative guidelines to assist in choosing housanes that will be oxidizable, (c) the spin and charge distribution of the cation radical that was selected for the present investigation, and (d) a rationale for the observed regioselectivity.

Results and Discussion

Choice of Oxidizing Agent. A variety of methods have proven suitable for the oxidation of housanes.[5] We prefer to generate the oxidizing agent in situ via the electrochemical oxidation of tris(4-bromophenyl)amine (TBA, **14**).[6] In this manner, one can operate at a potential that is significantly less than that required for the direct oxidation of the substrate. For example, the amine (**14**) oxidizes at ~ +0.9 V versus a silver/silver nitrate reference electrode. In contrast, the 2-phenyl-substituted housane **1** displays its first oxidation peak at a potential of +1.3 V. Nevertheless, the arylamminium cation radical **14**$^{\bullet+}$ smoothly converts **1** to its cation radical and, subsequently, to products **4** and **5**. The apparent thermodynamic impasse is countered by the existence of at least one irreversible follow-up reaction that drains the equilibrium toward the products.[7] This general phenomenon allows products that might be oxidized under more harshly oxidizing conditions to be protected.

Oxidizability. With the tris(*p*-bromophenyl)amminium cation radical **14**$^{\bullet+}$ as the oxidant of choice, we considered it prudent to develop a qualitatively useful means to assess housane

(4) See, for example, the structures shown in: Wilson, R. M.; Danishefsky, S. J. *Acc. Chem. Res.* **2006**, *39*, 539−549.

(5) For example, see: (a) Cossy, J.; Belotti, D. *Tetrahedron* **2006**, *62*, 6459−6470; Floreancig, P. E. *Tetrahedron* **2006**, *62*, 6447−6594 (Symposium-in-Print Number 121). (b) Floreancig, P. E. *Synlett.* **2007**, 191−203. (c) Roth, H. D. In *Reactive Intermediate Chemistry*; Moss, R. A., Platz, M. S., Jones, M., Jr., Eds.; John Wiley & Sons: New York, 2004; Chapter 6, pp 205−272. (d) Moeller, K. D. *Tetrahedron* **2000**, *56*, 9527−9554. (e) Rinderhagen, H.; Waske, P. A.; Mattay, J. *Tetrahedron* **2006**, *62*, 6589−6593. (f) Adam, W.; Corma, A.; Miranda, M. A.; Sabater-Picot, M.-J.; Sahin, C. *J. Am. Chem. Soc.* **1996**, *118*, 2380−2386. (g) Booker-Milburn, K. I.; Cox, B.; Grady, M.; Halley, F.; Marrison, S. *Tetrahedron Lett.* **2000**, *41*, 4651−4655. (h) Takemoto, Y.; Furuse, S.-I.; Hayase, H.; Echigo, T.; Iwata, C.; Tanaka, T.; Ibuka, T. *Chem. Commun.* **1999**, 2515−2516. (i) Bauld, N. L.; Bellville, D. J.; Harirchian, B.; Lorenz, K. T.; Pabon, R. A., Jr.; Reynolds, D. W.; Wirth, D. D.; Chiou, H. S.; Marsh, B. K. *Acc. Chem. Res.* **1987**, *20*, 371−378.

(6) (a) Mayers, B. T.; Fry, A. J. *Org. Lett.* **2006**, *8*, 411−414 and 1253. (b) Wend, R.; Steckhan, E. *Electrochem. Acta* **1997**, *42*, 2027−2039. (c) Dapperheld, S.; Steckhan, E. *Angew. Chem.* **1982**, *94*, 785. (d) Platen, M.; Steckhan, E. *Chem. Ber.* **1984**, *117*, 1679−1694. (e) Dapperheld, S.; Steckhan, E.; Brinkhaus, K. H. G.; Esch, T. *Chem. Ber.* **1991**, *124*, 2557−2567.

(7) Miranda, J.; Wade, C.; Little, R. D. *J. Org. Chem.* **2005**, *70*, 8017−8026.

TABLE 1. Calculated HOMO Energies for a Series of Housanes

Entry		E(HOMO) eV; B3LYP/6-31G(d)	Entry		E(HOMO) eV; B3LYP/6-31G(d)
1	 **15**	–6.83 [$E_{1/2}$(ox; ref. 5f) ~ 1.9V]	4	 **1**	–6.20 [E_p(ox; ref. 1) ~ 1.5V]
2	 **16**	–6.59			
3	 **17**	–6.37	5	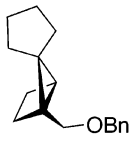 **18**	–6.48

SCHEME 4. Synthesis of Housane 18

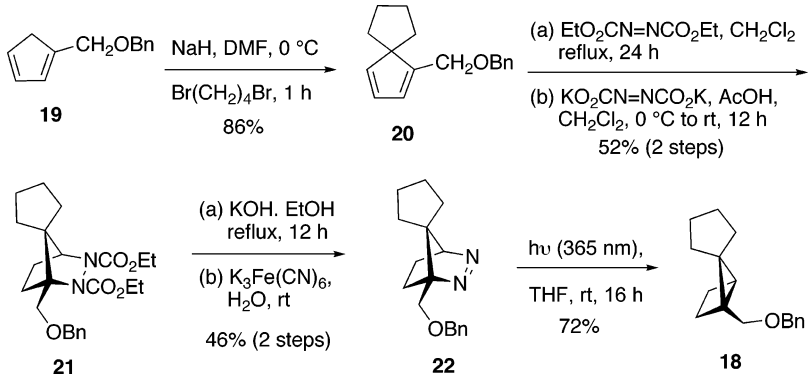

oxidizability prior to spending the time and effort required to synthesize a substrate. We wanted to be confident that the system we selected would not be too difficult to oxidize. We know, for example, that the parent housane **15** is not oxidized by **14**$^{\bullet+}$, while the 2-aryl-substituted housanes **1**−**3** are easily oxidized. Given the correlation between HOMO energies and oxidizability, we have found it convenient to calculate their energies and to correlate the calculated values with measured oxidation potential for housanes whose oxidations we, or others, have investigated.[8]

Table 1 illustrates the HOMO energies for a series of housanes calculated at the B3LYP/6-31G(d) level of theory.[9] Since the parent housane, bicyclo[2.1.0]pentane (**15**), has been shown to be inert to **14**$^{\bullet+}$ while the bridgehead methyl-substituted housane **16** undergoes oxidation,[5f] we conclude that, for housanes whose HOMO energy is equal to or more positive than −6.59 eV, **14**$^{\bullet+}$ will be a suitable oxidizing agent. Somewhere between there and approximately −6.9 eV, it will fail. The influence of a second bridgehead methyl group is to raise the HOMO energy from −6.59 to −6.37, indicating that **17** will be easier to oxidize than **16**, a conclusion that accords nicely with experiment.[5f] The HOMO energy for the analogous 2-phenyl-substituted housane **1** is still more positive (−6.20). Thus it ought to be the easiest to oxidize of the systems portrayed, and this is observed to be true.[1] The last entry in the table is monoalkylated and ought, therefore, to be oxidizable by **14**$^{\bullet+}$. The calculated HOMO energy supports this notion, so we felt confident to select **18** as a substrate for the present investigation.

Synthesis of 2-Benzyloxymethylhousane 18. On the basis of the ideas discussed in the previous section and in an effort to impose a bias on the directionality of the rearrangement step, we elected to synthesize housane **18** (Scheme 4), a system whose bridgehead substituents are different. To do so, we capitalized upon the facility of substituted cyclopentadienes to undergo 1,5 hydrogen shifts.[10] Thus, the product from alkylation of the cyclopentadienyl anion with benzyl chloromethyl ether readily undergoes sigmatropic rearrangement to afford **19**. Subsequent treatment with sodium hydride and 1,4-dibromobutane leads smoothly to the spirocyclic diene **20**. Its conversion to diazene **22** followed a standard protocol involving Diels−Alder cycloaddition with diethyl azodicarboxylate, reduction to the back bond of the resulting adduct, and transformation of the biscarbamate linkage to the diazene. When photolyzed, **22** loses nitrogen and efficiently leads to the desired housane **18**.

Catalytic, Electrochemically Mediated Oxidation of

(8) Adam, W.; Heidenfelder, T. *Chem. Soc. Rev.* **1999**, *28*, 359−366.

(9) (a) All calculations performed at UCSB used the SPARTAN '04 Macintosh software package, while those performed at UCD used the *GAUSSIAN03* suite of programs (Frisch, M. J.; et al. *Gaussian 03*; Gaussian, Inc.: Wallingford, CT, 2003). (b) Geometries and HOMO energies for the systems illustrated in Table 1 were calculated at the HF/3-21G(d), HF/6-31G(d), and B3LYP/6-31G(d) levels of theory. The trends in HOMO energies vary slightly with different levels of theory, but in a manner that does not change any of our conclusions. See Supporting Information for additional details on all of these calculations, including pictures of the computed HOMOs.

(10) Yang, Y.-R.; Li, W.-D. Z. *J. Org. Chem.* **2005**, *70*, 8224−8227.

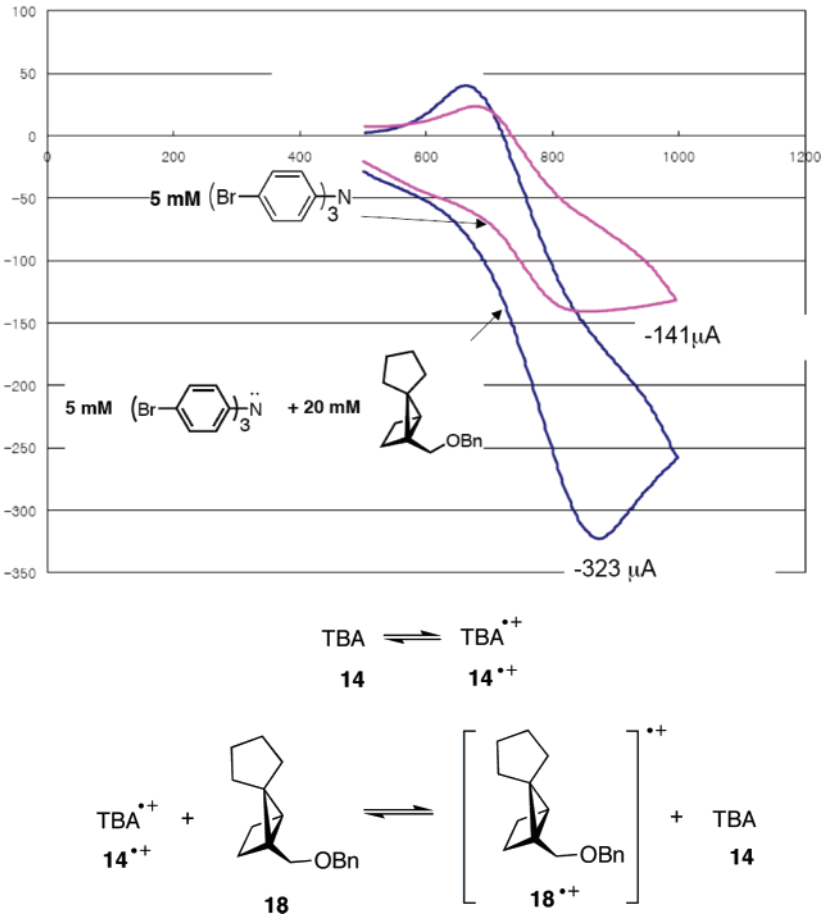

FIGURE 1. Cyclic voltammograms showing the TBA/TBA cation radical redox couple (pink) and the existence of a catalytic current when the substrate (**18**) is added (blue curve). Glassy carbon anode, Pt wire cathode, $Ag/AgNO_3$ reference electrode, 0.1 M *n*-Bu_4NBF_4 supporting electrolyte in acetonitrile solvent, 200 mV/s scan rate.

Housane 18: Rearrangement with Exceptionally High Regioselectivity. Our plan called for the use of **14**$^{\bullet+}$ to mediate the oxidation of housane **18**. The cyclic voltammogram for the TBA/TBA cation radical couple is displayed in pink in Figure 1. When the benzyloxymethyl-substituted housane **18** is added and the scan repeated, there is an increase in current flow that is attributable to a so-called catalytic current (note the blue curve).[11] Its appearance is an excellent indicator that the amminium cation radical is able to oxidize the housane and return the mediator to the original redox couple, as illustrated by the equations accompanying Figure 1.

The preparative scale oxidation of **18** was conveniently carried out in a beaker-style cell that was fitted with a carbon cathode (reticulated vitreous carbon) and a platinum anode. The potential was set to +0.88 V in order to oxidize the 10 mol % of TBA that was dissolved in acetonitrile, rather than the housane; the course of the reaction was monitored by TLC.[12] We were delighted to discover the formation of a single product in a 66% isolated yield (89% based upon recovered starting material) whose spectral data are consistent with the bridgehead substituted bicyclic alkene **23**. Thus, in contrast with systems we had previously studied (vide supra), the rearrangement of **18** proved to be highly regioselective; no evidence for the formation of a regioisomeric adduct was obtained.[13]

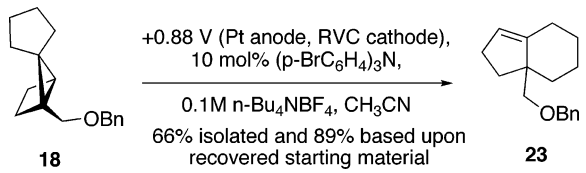

Characterization of the Intermediate and the Rearrangement Pathway. DFT calculations (B3LYP/6-31G(d)) and the resulting image shown in Figure 2 show that the HOMO for housane **18** is located on *both* the benzyloxymethyl and strained σ framework of the molecule.[9] The computed spin density surface for the ring-opened cation radical shows clearly that the unpaired spin resides on the side that is distal to the substituent, while the corresponding electrostatic potential map indicates that the side bearing the substituent is more positive, suggesting that the hole resides proximal to the substituent.

One mechanism that emerges from these considerations is illustrated in Scheme 5. The process begins with the oxidation

(11) (a) Steckhan, E. *Angew. Chem.* **1986**, *98*, 681−699. (b) Simonet, J.; Pilard, J.-F. Electrogenerated Reagents. In *Organic Electrochemistry*, 4th ed.; Lund, H., Hammerich, O., Eds.; Marcel Dekker: New York, 2001; Chapter 29. (c) Little, R. D.; Moeller, K. D. *Interface* **2002**, *11*, 36−42.

(12) The use of 20 mol % of the mediator leads to a significant rate increase, thereby allowing the complete consumption of the starting material in 2 h or less.

(13) Interestingly, GCMS analysis shows that heating **18** to 300 °C for 20 min affords *both* regioisomers. In the thermal process, the major product corresponds to the isomer that is not observed electrochemically.

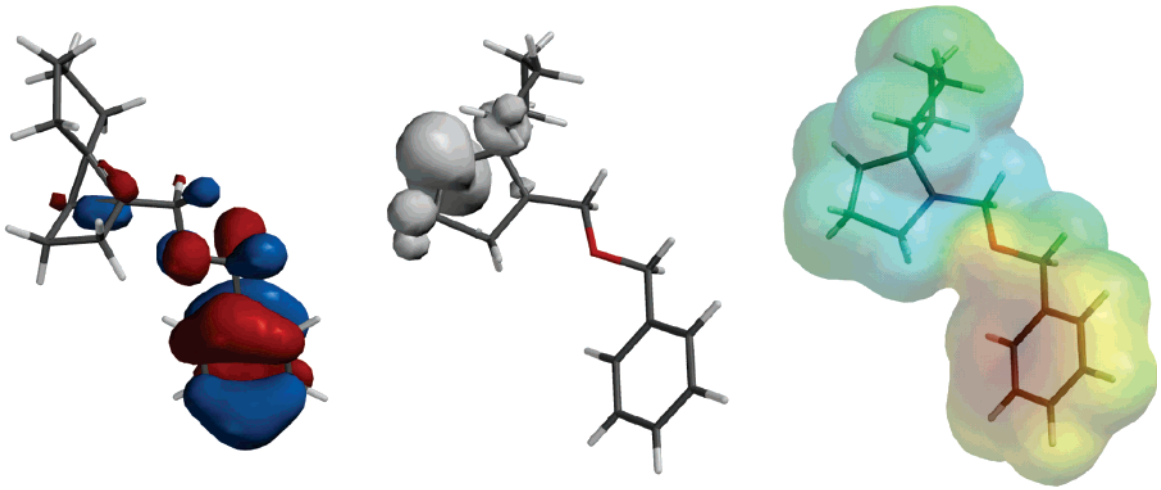

FIGURE 2. Left: HOMO for **18** determined at the B3LYP/6-31G(d) level of theory. Middle: Spin density for the cation radical (HF/3-21G(d)) derived from **18**. Right: Electrostatic potential map for the cation radical (HF/3-21G(d)).

SCHEME 5. Alternative Mechanistic Hypotheses for the Conversion of 18 to 23

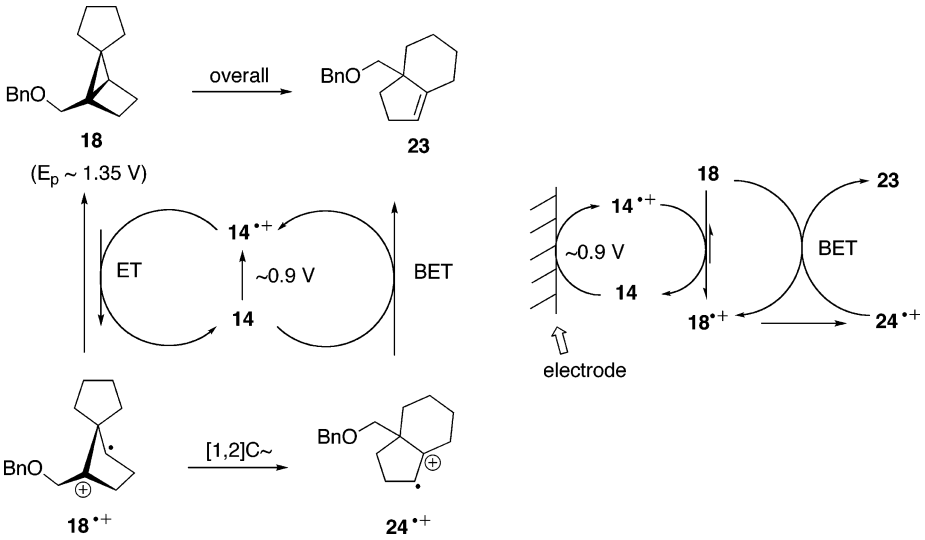

of the mediator TBA (**14**) at ~0.9 V to afford the TBA cation radical, **14**$^{\bullet+}$. It subsequently oxidizes the substrate **18** and regenerates TBA (**14**). The observation of a catalytic current supports the existence of this sequence (see Figure 1). One or more follow-up transformations are required to drive the unfavorable equilibrium that is established during this electron transfer (ET) step. We suggest that either the [1,2] carbon migration of the housane cation radical **18**$^{\bullet+}$ to afford the (4.3.0) cation radical **24**$^{\bullet+}$ and/or the subsequent back electron transfer (BET) from TBA to **24**$^{\bullet+}$ fulfill this need while also leading to the product **23** and regenerating the oxidizing agent, **14**$^{\bullet+}$. An alternative BET pathway posits that the starting material, **18**, rather than **14** provides the electron to **24**$^{\bullet+}$ to afford **23** and regenerate **18**$^{\bullet+}$ (shown on the right side of Scheme 5). At this time, we do not have evidence to favor either of these options.

Transition structures for the rearrangement step were generated at both the Hartree−Fock/3-21G(d) and density functional levels of theory (B3LYP/6-31G(d)).[9,14] Each level of theory leads to the same conclusion; that is, the rearrangement is best characterized as a [1,2] carbon shift toward an electron-deficient site, and migration toward the substituent-bearing carbon is much preferred over the alternative pathway. At the B3LYP/6-31G(d) level, for example, the activation barrier is ~7 kcal/mol for the distal pathway, while the proximal pathway is nearly barrierless. Similarly, single point energy calculations on the B3LYP/6-31G(d) structures using CCSD/6-31G(d) suggest that the barrier for the distal pathway is ~9 kcal/mol and that for the proximal pathway is again only a fraction of a kcal/mol.[14] In keeping with the proposed mechanism, this significant

(14) Geometries for structures involved in the rearrangement were optimized using the B3LYP/6-31G(d) method (Becke, A. D. *J. Chem. Phys.* **1993**, *98*, 5648−5652; Becke, A. D. *J. Chem. Phys.* **1993**, *98*, 1372−1377; Lee, C.; Yang, W.; Parr, R. G. *Phys. Rev. B* **1988**, *37*, 785−789; Stephens, P. J.; Devlin, F. J.; Chabalowski, C. F.; Frisch, M. J. *J. Phys. Chem.* **1994**, *98*, 11623−11627) on a model system with the benzyl group replaced by a methyl group. All structures were characterized by frequency calculations. Intrinsic reaction coordinate (IRC) calculations (Gonzalez, C.; Schlegel, H. B. *J. Phys. Chem.* **1990**, *94*, 5523−5527; Fukui, K. *Acc. Chem. Res.* **1981**, *14*, 363−368) were also used to characterize transition structures. Note that, as a test of this methodology, we attempted to predict the major product without prior knowledge of the experimental result; in this case, the prediction proved to be correct. CCSD/6-31G(d) (Scuseria, G. E.; Schaefer, H. F., III. *J. Chem. Phys.* **1989**, *90*, 3700−3703) single point calculations were also performed. See Supporting Information for additional details.

preference is likely to be due to the ability of an alkyl substituent to better stabilize a positive charge than an unpaired electron.

An alternative rationale for the experimentally observed regioselectivity posits that, like the cation radicals derived from the 2-aryl-substituted housanes **1**−**3**, the aryl unit is not an innocent bystander. It could, for example, bridge to stabilize a positive charge located at C-1 in the manner illustrated by structure **25**.[15] Subsequent Wagner−Meerwein rearrangement would re-establish aromaticity and generate structure **24**$^{\bullet+}$ (Scheme 6). While additional experiments must be performed to formally assess the viability of this suggestion, our quantum calculations show that this type of bridging is not required to explain the regiochemical preference.

SCHEME 6. Alternative Mechanistic Pathway

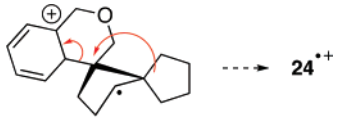

25

Concluding Remarks

The utility of catalytic electrochemically mediated processes as well as the application of simple quantum calculations to the implementation of the chemistry described herein has been demonstrated. The insight gained during these investigations promises to be of utility in designing substrates that will allow the housane-derived cation radical rearrangement reaction to be applied to the synthesis of specific structures, particularly, to those of natural products. Our efforts to apply the chemistry in this manner will be described in due course.

Experimental Section

1-Benzyloxymethyl-1,3-cyclopentadiene 19. To a stirred suspension of NaH (60% oil, 2.40 g, 60.05 mmol) in dry THF (40 mL) was added slowly a solution of freshly distilled cyclopentadiene (4.01 mL, 60.0 mmol) in THF (20 mL) over 20 min at −10 °C. After additional stirring for 30 min, the resulting purple reaction mixture was cooled to −70 °C, and then a solution of benzyl chloromethyl ether (10.01 mL, 72.0 mmol) in THF (20 mL) was added slowly to the reaction vessel over 20 min. The resulting reaction mixture was warmed to −50 °C and stirred at that temperature for 40 min, and allowed to warm gradually to 0 °C, quenched with saturated aqueous NH_4Cl (50 mL), and stirred for an additional 1 h. The organic layer was separated, and the aqueous layer was extracted with ether (5 × 100 mL). The combined organic layers were washed with water (2 × 100 mL) and brine (2 × 100 mL), dried over anhydrous sodium sulfate, filtered, and concentrated under reduced pressure at room temperature. The crude product was purified by flash chromatography on silica gel (petroleum ether/Et_2O 50:1, R_f = 0.23, UV, vanillin) to afford the alkylated product **19** as a yellow liquid (5.37 g, 28.9 mmol, 48%). ^{1}H NMR data matched the literature values.[10]

1-(Benzyloxymethyl)spiro[4.4]nona-1,3-diene 20. To a stirred suspension of NaH (60% oil, 2.02 g, 50.62 mmol) in dry DMF (40 mL) was added slowly a solution of the cyclopentadiene derivative **19** (4.287 g, 23.01 mmol) and 1,4-dibromobutane (3 mL, 25.32 mmol) in DMF (15 mL) keeping the temperature of the reaction mixture below 0 °C. The reaction was stirred for 1 h at 0 °C, quenched with saturated aqueous NH_4Cl (50 mL), and diluted with ether (100 mL). The organic layer was separated, and the aqueous layer was extracted with ether (5 × 75 mL). The combined organic portions were washed with brine (3 × 100 mL), dried over anhydrous sodium sulfate, filtered, and concentrated under reduced pressure. The crude product was purified by flash chromatography on silica gel (petroleum ether/EtOAc 100:1, R_f = 0.25, UV, vanillin) to afford **20** as a yellow liquid (4.76 g, 19.85 mmol, 86%). Additional purification could be achieved by using HPLC (5 micron silica, 10 mm i.d. × 25 cm), at a flow rate of 1.3 mL/min using hexane as the eluant: IR (neat) ν_{max} 3031, 2951, 2862, 1452, 1089, 1070, 737, 698 cm^{-1}; ^{1}H NMR (400 MHz, $CDCl_3$) δ 1.76−2.00 (m, 8H), 4.27 (s, 2H), 4.52 (s, 2H), 6.23 (dd, 1H), 6.27 (d, 1H), 6.48 (dd, 1H), 7.27−7.40 (m, 5H); ^{13}C NMR (400 MHz, $CDCl_3$) δ 22.9, 26.3, 31.8, 32.5, 63.8, 72.1, 127.7, 127.9, 128.4, 128.6, 138.8, 145.5, 150.1; LRMS (EI) *m*/*z* 240 (M^+, 12), 149 (20), 134 (59), 121 (50), 91 (100); HRMS (EI) *m*/*z* found 240.1508, calcd 240.1514 for $C_{17}H_{20}O$.

Diethyl 1-(Benzyloxymethyl)-2,3-diazaspiro[bicyclo[2.2.1]-heptane-7,1′-cyclopentane]-2,3-dicarboxylate (Biscarbamate 21). The spirocyclopentyl diene derivative **20** (2.0 g, 8.32 mmol) and diethyl azodicarboxylate (4.05 mL, 24.96 mmol) were dissolved in dry CH_2Cl_2 (80 mL), and the resulting mixture was brought to reflux with magnetic stirring for 24 h. The orange reaction mixture was cooled to room temperature and diluted with CH_2Cl_2 (50 mL), followed by the addition of dipotassium azodicarboxylate (16.13 g, 83.2 mmol). The reaction vessel was fitted with an addition funnel and an overhead stirrer. The mixture was cooled to 0 ×bcC, and diimide was generated in situ by the dropwise addition of glacial acetic acid (5.9 mL, 104 mmol) for 30 min. Vigorous evolution of gas occurred during the entire course of the addition. The mixture was gradually warmed to room temperature and stirred for 12 h. The solids were removed by filtration, and the remaining solids were washed with CH_2Cl_2 (200 mL). The solvent was evaporated under reduced pressure at room temperature and neutralized with saturated aqueous $NaHCO_3$. The layers were separated, and the aqueous layer was extracted with CH_2Cl_2 (75 mL × 5). The combined organic portions were washed with brine (100 mL × 2), dried over anhydrous Na_2SO_4, and concentrated under reduced pressure. The crude product was purified by flash chromatography on silica gel (petroleum ether/Et_2O 6:4, R_f = 0.30, UV, vanillin) to provide the biscarbamate **21** as a colorless liquid (1.80 g, 4.33 mmol, 52%): ^{1}H NMR (400 MHz, $CDCl_3$) δ 1.10−1.30 (m, 8H), 1.34−1.38 (m, 1H), 1.40−1.62 (m, 3H), 1.64−1.78 (m, 3H), 1.80−1.99 (m, 3H), 3.94−4.02 (m, 1H), 4.16−4.30 (m, 6H), 4.49−4.60 (m, 2H), 7.24−7.40 (m, 5H).

1-(Benzyloxymethyl)-2,3-diazaspiro[bicyclo[2.2.1]hept[2]ene-7,1′-cyclopentane] (Benzyloxymethyldiazene 22). The biscarbamate **21** (1.80 g, 4.33 mmol) was dissolved in EtOH (135 mL), the solution was degassed with argon for 20 min, and KOH (4.88 g, 87.0 mmol) was added. The resulting mixture was brought to reflux for 12 h. The reaction mixture was cooled to room temperature and diluted with EtOH (50 mL), followed by removing reflux condenser. After cooling to 0 °C, a solution of $K_3Fe(CN)_6$ (14.27 g, 43.34 mmol) in water (80 mL) was added slowly via addition funnel over a period of 1 h, and the mixture was stirred for 12 h at room temperature. TLC showed that Cu(I) test for the resulting diazene was positive. After the mixture was diluted with water (50 mL), the product was extracted with Et_2O (100 mL × 6) and dried over anhydrous $MgSO_4$. The crude product was obtained upon concentration under reduced pressure. Purification by flash chromatography on silica gel (petroleum ether/Et_2O 7:4, R_f = 0.28, Cu-(I) stain, UV, vanillin) to afford the diazene **22** as a colorless liquid (537 mg, 1.99 mmol, 46%): IR (neat) ν_{max} 3029, 2950, 2865, 1492, 1454, 1097, 737, 698 cm^{-1}; ^{1}H NMR (400 MHz, $CDCl_3$) δ 0.94−1.01 (m, 2H), 1.18−1.22 (m, 1H), 1.32−1.60 (m, 7H), 1.66−1.75 (m, 2H), 4.09 (d, J = 10.44 Hz, 1H), 4.30 (d, J = 10.44 Hz, 1H), 4.70 (d, J = 6.14 Hz, 2H), 4.76 (t, J = 2.92 Hz), 7.29−7.89 (m, 5H); ^{13}C NMR (400 MHz, $CDCl_3$) δ 20.5, 23.3, 25.9, 26.0, 28.3, 28.5, 64.2, 68.0, 73.9, 86.2, 88.8, 127.6, 127.7, 128.5, 138.4; LRMS

(15) Stabilization of an incipient or fully formed cation (or radical) could also be achieved through participation by the ether oxygen. We have no evidence to favor or disfavor this possibility.

(ESI+/TOF) *m/z* 271 $[M + H]^+$, 293 $[M + Na]^+$, 563 $[2M + Na]^+$; HRMS found 293.1626, calcd 293.1624 for $C_{17}H_{22}N_2ONa$.

1-(Benzyloxymethyl)spiro[bicyclo[2.1.0]pentane-5,1′-cyclopentane] (Benzyloxymethylhousane 18). The diazene **22** (356 mg, 1.31 mmol) was weighed into a 50 mL Pyrex round-bottomed flask and dissolved in dry THF (15 mL). The solution was degassed by bubbling argon through it for 20 min. Then, the solution was irradiated with UV light of 365 nm from a UV hand lamp placed adjacent to the flask, and the reaction was followed up by TLC. After 16 h, the diazene was consumed and the solvent was evaporated under reduced pressure at room temperature. The crude product was chromatographed on silica gel (petroleum ether/Et_2O 50:1, $R_f = 0.21$, UV, vanillin) to afford the benzyloxymethylhousane **18** as a colorless liquid (356 mg, 0.94 mmol, 72%): IR (neat) ν_{max} 3027, 2940, 2858, 1452, 1089, 1069, 733, 696 cm^{-1}; ^1H NMR (400 MHz, $CDCl_3$) δ 1.13 (m, 1H), 1.34−1.35 (m, 2H), 1.55−1.77 (m, 8H), 2.01−2.18 (m, 2H), 3.53 (d, $J = 11.21$ Hz, 1H), 3.67 (d, $J = 11.21$ Hz, 1H), 4.47 (d, $J = 12.13$ Hz, 1H), 4.58 (d, $J = 12.13$ Hz, 1H), 7.29−7.35 (m, 5H); ^{13}C NMR (400 MHz, $CDCl_3$) δ 18.6, 23.7, 24.5, 25.9, 26.8, 29.2, 31.2, 31.5, 36.2, 71.6, 72.4, 127.6, 127.8, 128.5, 139.1; LRMS (EI) *m/z* 242, 151, 134, 121, 108, 91 (base peak); HRMS found 242.1671, calcd 242.1671 for $C_{17}H_{22}O$.

Cyclic Voltammetry. Cyclic voltammograms were recorded in a single cell fitted with three electrodes. A glassy carbon disc electrode (0.033 cm^2 surface area) was used as a working electrode, and a platinum wire (0.6 cm^2 surface area) was used as a counter electrode. The potential was recorded with the reference electrode Ag/0.01 M $AgNO_3$ immersed in a 0.1 M solution of *n*-Bu_4NBF_4 in CH_3CN that was separated from the medium by a Vycor membrane. Its potential was +0.35 V versus the aqueous saturated calomel electrode (SCE). All solutions were deoxygenated with a stream of argon for 20 min before each experiment. A scan rate of 200 mV/s was used. Cyclic voltammetry (CV) was performed using a computer-controlled potentiostat (Cypress voltammetric system CS 1200), and data were collected using the software available from Cypress (version 1.5.5) and exported to an Excel Microsoft worksheet.

General Procedure for Preparative Indirect Electrolysis. All preparative electrolyses were carried out in an undivided cell fitted with a platinum anode (1 cm^2 surface area) as a working electrode and a reticulated vitreous carbon (RVC) electrode as a counter electrode. A Ag/0.01 M $AgNO_3$ reference electrode used for the electrolyses had a potential of +0.35 V versus the aqueous calomel electrode (SCE) at 25 °C. The separation between each of the electrodes was ca. 0.5 cm. The potentials of all reactions were controlled by a potentiostat, and the amount of charge passed was monitored using a coulometer. In a preparative cell, a 0.1 M solution of *n*-Bu_4NBF_4 in CH_3CN (15 mL) was added. All electrodes were fitted in the cell, and then the solution was deoxygenated by bubbling argon through it for 20 min. A pre-electrolysis was conducted at constant potential of 880 mV until the current value dropped to ca. 0.5 mA. We routinely carried out pre-electrolyses in order to ensure the absence of any redox-active materials at the time when the substrate was added to the reaction medium.

Housane **18** (100 mg, 0.413 mmol) and 10 mol % of tris(4-bromophenyl)amine (20 mg, 0.041 mmol) were added to the solution. When a potential of +880 mV was applied to the cell, the current flow increased to 7.7 mA, and a blue color appeared on the surface of the platinum electrode, indicating the oxidation of the mediator. The reaction was monitored by TLC; the electrolysis was stopped after the coulometer indicated that 1 F/mol had passed. The dark yellow solution was poured into an Erlenmeyer flask containing water (15 mL), and the separated aqueous layer was extracted with Et_2O (40 mL × 5). The combined organic portions were washed with brine (50 mL × 2), dried over $MgSO_4$, and concentrated under reduced pressure at room temperature. The crude product was purified by flash chromatography on Si_2O (petroleum ether/Et_2O 50:1, $R_f = 0.39$, UV, vanillin) to afford the bicyclononene **23** as a colorless liquid (66 mg, 0.27 mmol, 66%). The starting material (23 mg, 0.095 mmol, 23%) was also recovered and could be reused if desired.

7a-(Benzyloxymethyl)-2,4,5,6,7,7a-hexahydro-1*H*-indene (Benzyloxymethyl Bicyclononene 23): IR (neat) ν_{max} 3033, 2927, 2850, 1453, 1093, 1027, 908, 732, 696 cm^{-1}; ^1H NMR (400 MHz, $CDCl_3$) δ 1.10−1.27 (m, 2H), 1.39−1.55 (m, 3H), 1.74−1.78 (m, 1H), 1.88−1.98 (m, 1H), 2.11−2.22 (m, 3H), 2.25−2.35 (m, 2H), 3.27 (d, $J = 8.91$ Hz, 1H), 3.44 (d, $J = 8.91$ Hz, 1H), 4.51 (d, $J = 12.44$ Hz, 1H), 4.58 (d, $J = 12.44$ Hz, 1H), 5.33 (q, $J = 2.15$, 1H), 7.28−7.36 (m, 5H); ^{13}C NMR (400 MHz, $CDCl_3$) δ 15.5, 22.9, 27.1, 27.7, 29.9, 36.7, 50.7, 66.1, 72.4, 73.4, 122.6, 127.6, 128.5, 139.2, 146.2; LRMS (EI) *m/z* 241 (3), 199 (7), 151 (21), 121 (100), 91 (57); (CI/CH_4) *m/z* 363 (5), 269 (4), 243 (10), 241 (9), 151 (28), 135 (80), 121 (100); HRMS (CI /CH_4) found 243.1758, calcd 243.1749 for $[C_{17}H_{22}O + H]^+$.

Acknowledgment. We thank the Petroleum Research Fund administered by the American Chemical Society (ACS PRF# 43443-AC1) for its support of this research. The research at UCD was supported in part by the National Science Foundation through the Pittsburgh Supercomputer Center.

Supporting Information Available: Additional information for compounds **18** (^1H and ^{13}C) and **20** (^1H and ^{13}C), **21** (^1H), **22** (^1H and ^{13}C), and **23** (^1H and ^{13}C), a CV curve for housane **20** and the product, **23**, as well as additional details concerning the calculations. This material is available free of charge via the Internet at http://pubs.acs.org.

JO070190X